

2004

Nanodosimetric cluster size distributions of therapeutic proton beams

A. J. Wroe

University of Wollongong

R. Schulte

Loma Linda University Medical Centre, USA

V. Bashkirov

Loma Linda University Medical Centre, USA

Anatoly B. Rosenfeld

University of Wollongong, anatoly_rozenfeld@uow.edu.au

B. Grosswendt

Physikalisch-Technische Bundesanstalt, Germany

Publication Details

This paper originally appeared as: Wroe, AJ, Shulte, R, Bashkirov, V et al, Nanodosimetric cluster size distributions of therapeutic proton beams, IEEE Nuclear Science Symposium Conference Record, 16-22 October 2004, vol 3, 1857-1861. Copyright IEEE 2004.

Nanodosimetric cluster size distributions of therapeutic proton beams

Andrew J. Wroe, *Student Member IEEE*, Reinhard Schulte, Vladimir Bashkirov, Anatoly B. Rosenfeld, *Senior Member IEEE*, Bernd Grosswendt

Abstract—As we move into the new millennium, it is important that we improve our understanding of radiation effects on humans and nanoelectronic systems. This understanding is essential in a number of areas including radiation therapy for cancer treatment and extended human presence in outer space. Nanodosimetry in low-pressure gases enables measurement of the energy deposition of ionizing radiation on a scale equivalent to the dimensions of the DNA molecule. This is extremely important for not only biological applications but also electronic applications, as the effect of radiation on nanoelectronics needs to be determined before they are installed and deployed in complex radiation fields. However, before nanodosimetry can be widely applied, further investigation is required to link the output of gas-based nanodosimeters to the actual effect of the radiation on a biological or electronic system. The purpose of this research is to conduct nanodosimetric measurements of proton radiation fields at the proton accelerator of Loma Linda University Medical Center (LLUMC) and to develop a Monte Carlo simulation system to validate and support further developments of experimental nanodosimetry. To achieve this, measured ion cluster size distributions are compared to the output from the Monte Carlo simulation system that simulates the characteristics of the LLUMC beam line and the performance of the nanodosimeter installed on one of LLUMC's proton research beam lines.

I. INTRODUCTION

Presently the standard for measuring radiation is absorbed dose, which gives us a macroscopic value for the energy deposited by radiation within a volume of a given mass. However, as our understanding of cellular function and DNA grows it is desirable to measure the effects of radiation on a DNA level, as this could provide us with a much more

accurate assessment of the biological effect of various radiation fields.

One such area where this improved understanding would be advantageous is in the use of radiation to treat cancer. Projections are that one in three people will suffer from this terrible disease or side effects of its treatment at one stage in their life [1]. Due to the deleterious effects that cancer and current treatment forms are having on the human population, better treatment techniques are constantly being sought. One of the most exciting and promising of these is proton therapy.

To gain maximum benefit from proton therapy, extensive treatment planning needs to be carried out to optimize beam energies and angles for each individual patient and localize the treatment. However, the interactions of protons are considerably more complex than those of X-rays and electrons associated with conventional radiotherapy, resulting in a more complex relationship between dose and biomedical effects. In this instance it is desirable to measure the effects of radiation on a DNA level as this could provide us with a much more accurate assessment of the biological effect of the treatment radiation.

Current proton treatment planning is based on macroscopic pencil beam algorithms that do not consider individual interactions of the charged particles and ignore the stochastic aspects of the energy deposition on the nanoscopic (DNA) level. This is an important determinant of the biological effectiveness of the radiation, which increases as the protons slow down in the patient. Current planning systems ignore this depth dependence. In order to make proton treatment planning more accurate, one should take the microscopic characteristics of proton radiation into account.

This research is centered on providing a more accurate theoretical means for determining the cluster size distribution on a nanoscopic or DNA level, by accurately reflecting the experimental radiation conditions. Once this system has been developed and verified using experimental methods and its accuracy assessed, it will be possible to include more complex homogeneous and heterogeneous structures into the theoretical model. This may then provide a means for better predicting radiation effects in radiation therapy or assess radiation risks in radiation protection applications.

Manuscript received October 4, 2004. Dr Schulte's research is supported by the National Medical Technology Testbed Inc. (NMTB) under the U.S. Department of the Army Medical Research Acquisition. Activity, Cooperative Agreement Number DAMD17-97-2-7016. Andrew Wroe is supported in part by the Australian Institute for Nuclear Science and Engineering.

A. J. Wroe and A. B. Rosenfeld are with the Centre for Medical Radiation Physics, University of Wollongong, Australia (telephone: 61-2-4221-5754, e-mail: ajw16@uow.edu.au, anatoly@uow.edu.au).

R. Schulte and V. Baskirov are with the Department of Radiation Medicine, Loma Linda University Medical Center, CA, USA (telephone: 01-909-558-4243 e-mail: rschulte@dominion.llumc.edu, vbashkirov@dominion.llumc.edu).

B. Grosswendt is with the Physikalisch-Technische Bundesanstalt (PTB), Braunschweig Germany (e-mail: Bernd.Grosswendt@ptb.de).

II. EXPERIMENTAL NANODOSIMETRY

The investigators at LLUMC, in collaboration with the Weizmann Institute of Science, have built and optimized two ion counting nanodosimeters [2, 3]. One of these nanodosimeters is situated on a research beam line at LLUMC and has been utilized in this research.

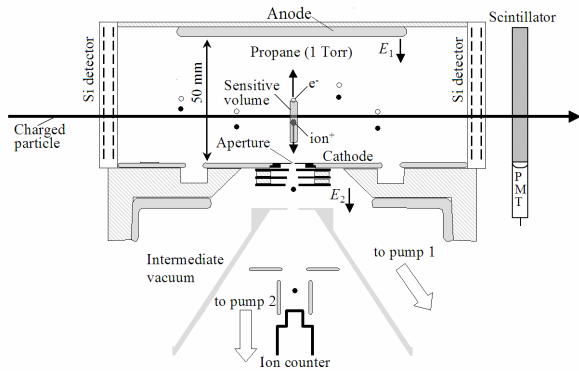


Fig. 1. Cross-section of the ion-counting nanodosimeter (ND) at LLUMC. The sensitive volume (SV) from which ionization ions are collected is shown as a shaded cylinder above the ND aperture. The field E_1 is defined by the voltage at the anode with respect to the cathode (ground). The field E_2 is defined by the voltages on the three electrodes below the ND aperture, the cone voltage, and the voltage on the first dynode of the ion counter. Pumps 1 and 2 (not shown) are turbomolecular pumps (VT 250 and VT 550, Varian) that generate the pressure gradient between the 1 Torr gas volume and the 5×10^{-5} Torr required for the ion counter.

The design of the nanodosimeter is shown in Fig. 1. The nanodosimeter detects positive ions, which are induced by the protons (or other charged particles) in a low-pressure propane gas. The use of the low gas pressure (1 Torr) allows scaling down a millimeter-size gas volume from which ions are collected to an equivalent tissue density volume of nanometer size (i.e., by a factor 10^6). The exact scaling factor also depends on mean free path length between ionizations, and for propane of 1 Torr, 1 mm in the lab system corresponds to about 3 nm in the tissue-equivalent unit-density system. Inside the nanodosimeter, a small needle-shaped sensitive volume (SV) is formed, which is defined by an electric field E_1 that drifts the radiation-induced positive ions toward a 1 mm diameter aperture at the bottom of the gas volume. An acceleration field E_2 accelerates the collected ions toward an ion counter, which is operated in vacuum. The nanodosimeter thus measures the number of ions induced per particle in a near-cylindrical, wall-less sensitive volume simulating a short segment of DNA and the surrounding water of about 5 nm in diameter (FWHM) and a length that can be selected with ion drift time cuts to be 2-50 nm. The quantity of interest for applications in radiation therapy and radiation protection is the frequency distribution of ion clusters formed in such a volume. It has been hypothesized that large clusters, despite being quite rare, are mainly responsible for irreparable DNA damage in a living cell and, therefore, determine the biological effectiveness of the radiation [3].

In this research, nanodosimetric cluster size distributions (CSDs) are measured using the ion-counting ND within a proton radiation field. We report here, on a radiation field that would comprise of a beam of 250MeV protons with $\sigma=40\text{keV}$, which was delivered from the accelerator to the nanodosimeter, passing beam modifying devices upstream from the nanodosimeter (Fig. 2). From a relatively inhomogeneous broad beam a homogeneous circular beam profile of 1cm radius was selected offline by using the particle track information from the built-in silicon strip detector tracking system (Fig. 1). Cluster size distributions were collected from a total number of 1.62×10^7 proton histories (Fig. 5) and compared with simulated distributions.

III. MONTE CARLO SIMULATIONS

Monte Carlo (MC) codes, once verified, provide a powerful tool to validate and improve experimental nanodosimetric systems and to provide additional data without performing time-consuming and expensive accelerator experiments. In this case, it is important to accurately simulate the experimental conditions present whilst taking measurements with the nanodosimeter in order to obtain an accurate result.

For these simulations it is important to obtain accurate information on the beam incident on the nanodosimeter. To achieve this, the GEANT4 Hadron Transport Toolkit [4, 5] was used to simulate the research beam line at LLUMC (Fig. 2.) and output the spectral and fluence distributions of protons as the beam enters the ND (Fig. 3 and Fig. 4). The beam modifying devices and regions that were simulated within the geometry module of this program included the evacuated beam line, secondary emission module (SEM), entrance and exit windows, air gaps between the SEM and ND, and two silicon strip detectors located at the entrance of the ND. Elements making up materials, utilized within the phantom geometry, would be defined by isotopic abundance. This provided the most accurate composition available and was obtained from an ICRU based program [6]. In order to match the conditions under which experimental cluster size distributions were obtained, the proton beam entering the beam modifying devices would have a radius of 10mm and an energy of 250MeV and $\sigma=40\text{keV}$. Simulations were conducted for 5 million incident protons to ensure good statistics.

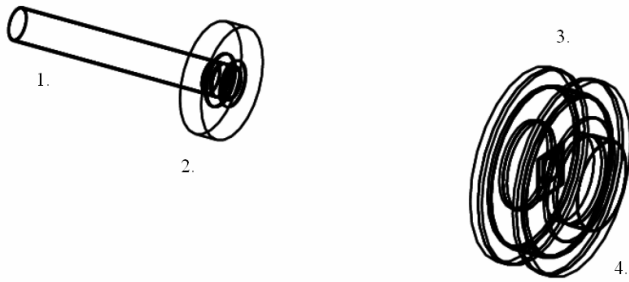


Fig. 2. The GEANT4 geometry used in simulating the LLUMC beam line. The components are 1. Evacuated beam pipe; 2. Secondary emission module complete with foils and exit window; 3. Si detector chamber complete with Si strip detector; 4. Entrance of the nanodosimeter.

As ionizations within a nanoscopic volume are to be measured and cluster size determined, it is imperative that it be possible to simulate electrons down to the ionization potential of the gas (11eV) in order to be as accurate as possible in our simulations. As a consequence, the GEANT4 program provides the energy spectra and fluence distribution of the beam incident onto the ND as two separate output files. These output files are used as initial history input for a special Monte Carlo code that has been developed by Dr. Bernd Grosswendt at PTB to simulate the performance of the nanodosimeter [2].

The specialized Monte Carlo code was written in Fortran and utilizes experimentally obtained cross sections to transport secondary electrons produced by the incident protons down to a cut-off value of 10eV (as the ionization energy for propane is 11eV). The geometry utilized within this program consists of a homogeneous propane gas of 1 Torr with an embedded sensitive volume in which the position and number of ions is registered. The dimensions and shape of the SV were chosen to match that of the experimental ND. As such, it simulates the internal conditions present within the ND. The output of this program was compared to the experimental results obtained using the ND for 250 MeV incident proton energies.

IV. RESULTS AND DISCUSSION

The results obtained by this research were collected as two separate sections that would reflect the output of the two separate Monte Carlo codes. Firstly, the fluence and energy distribution output files from the GEANT4 program would be obtained and reviewed. These files would then be utilized as input files to obtain a theoretical nanodosimetric spectra that would then be compared with experimental results obtained from the low pressure gas nanodosimeter situated a LLUMC.

A. Simulation of Beam Modifying Devices

The simulation of the beam modifying devices provided us with beam fluence and energy spectra data that would allow for an accurate assessment of the beam conditions entering the nanodosimeter (Fig. 3. and Fig. 4.).

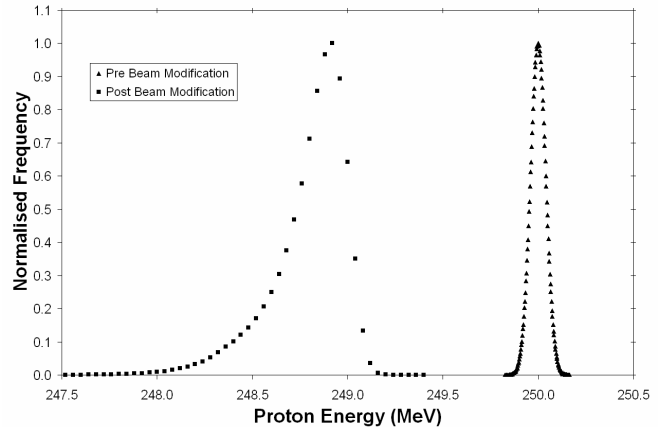


Fig. 3. Simulated energy distributions of the LLUMC proton beam before and after proceeding through the beam modifying devices. Distributions normalised to peak frequency.

In Fig 3. the energy spectra of the incident proton beam before traversing the beam modifying devices are shown to have a mean energy of 250MeV with $\sigma=40\text{keV}$, as per the experimental beam conditions at LLUMC. After traversing the beam modifying devices, the beam has lost energy and undergone a range straggling that has resulted in a non-symmetrical peak with a low energy tail. The mean proton energy is 248.9MeV with a FWHM of approximately 0.3MeV.

The GEANT4 Monte Carlo program would not only provide accurate peak information but also information regarding low energy protons. These low energy protons are present below the peak energy and range down to energies of only 2MeV. Whilst not in any great abundance, these low energy protons have an elevated LET that could lead to larger clusters within the SV of the nanodosimeter. In order to accurately assess the impact of these low energy protons, two energy spectra files were output from this program. The first file gave the peak energy spectra between 246MeV and 249.4MeV while the second gave the low energy spectra of all proton energies below 246MeV. Each of these separate energy spectra files would be utilized in separate nanodosimetry simulations of 10^7 histories to ensure good statistics for both. The nanodosimetric cluster frequency distributions from both would then undergo a weighted summation based upon the relative number of histories in each input file to supply the total theoretical cluster distribution.

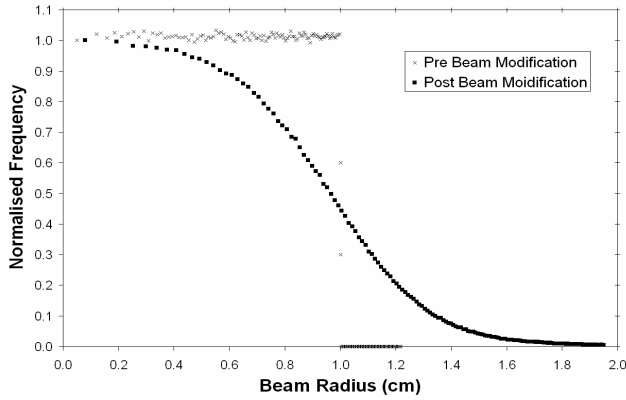


Fig. 4. Simulated radial distributions of the LLUMC proton beam before and after proceeding through the beam modifying devices. Distributions normalized to central bin frequency.

As per the experimental beam conditions, the incident beam prior to entering the beam modifying devices had a uniform profile and a radius of 1.0cm. Once passing through the beam modifying devices including SEM foils, air gap, nanodosimeter entrance window and Si strip detector, the beam has spread significantly and extends out to a radius of 1.0cm at FWHM. This fluence distribution would be used as the input for the nanodosimeter simulations.

B. Simulation of Nanodosimetric Cluster Distributions

Simulation of the response of the nanodosimeter would be carried out using a specially designed Monte Carlo code to simulate the performance of the ND. To attain accurate statistics, all simulations were run for 10^7 histories. This simulation program also had the feature of being able to evaluate the effect of secondary and Auger electrons by being able to include the transport of these particles as required.

Fig. 5 illustrates a comparison between experimental and theoretical cluster size distributions (transport of all secondary electrons considered) *including* zero-events (proton events without any ion detection in the SV). Fig. 6 displays a comparison between experimental and theoretical cluster size distributions *excluding* zero-events. It also shows the influence of different electron transport parameters investigated in the theoretical results.

The following results should be noted. The experimental cluster size distribution including zero events contains higher frequencies of non-zero cluster sizes than the simulated distribution. This is also reflected in the experimental mean cluster size of 8.78×10^{-3} compared to the theoretical mean cluster size of 4.53×10^{-3} ions. On the other hand, for the cluster size distributions excluding zero events (Fig. 6) excellent agreement is observed up to a cluster size of 9 ions when all secondary electrons are transported. Above cluster sizes of 9 ions, the experimental frequencies become progressively larger than the simulated frequencies as cluster size increases.

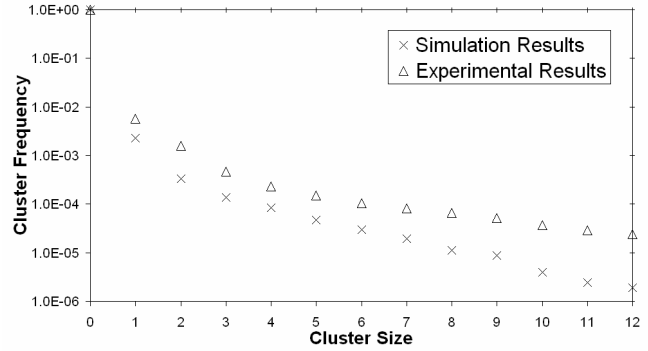


Fig. 5. Cluster size distribution comparisons for theoretical and experimental results. Distributions were normalized to the total number of events including zero events.

The higher frequency of non-zero events under experimental conditions could indicate that particles are entering the ND gas volume that are not accounted for in the simulation. The simulation only accounts for protons entering the gas volume and as such the source of the additional clusters could be secondary electrons produced in the upstream silicon strip detector as well as neutron contamination of the beam. It is likely that secondary electrons are the main contributor of additional clusters of smaller size (less than 10 ions), since the experimental and theoretical distributions excluding zero events agree very well in this range. Increasing discrepancy of the conditional cluster size distributions for >9 ions may be due to neutron contamination, since these would preferentially contribute large clusters, but could also be due to a rare ion multiplication mechanism in the ion acceleration channel below the ND aperture as suggested by Garty et al. [2].

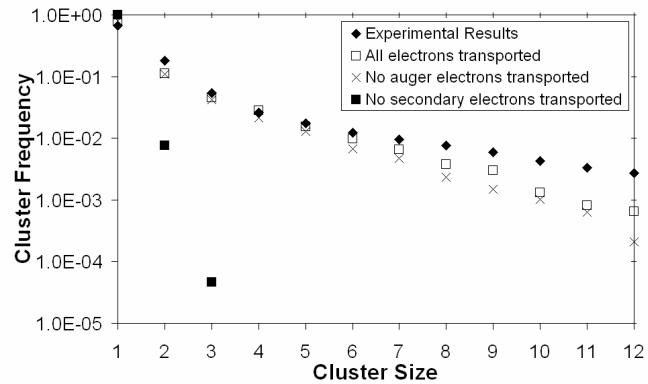


Fig. 6. Cluster size distribution comparisons for simulations with different electron transport parameters. The different electron transport parameters provide information on the importance of secondary electrons to the cluster size distribution. Distributions were normalized to the total number of events with at least one ion (cluster size ≥ 1).

The effect of secondary and Auger electron generation and transport in the gas volume was also investigated and the results are displayed in Fig 6. It is clear that secondary electron interactions within the SV contribute significantly to cluster

sizes larger than one ion with only small cluster sizes deriving from direct proton ionization within the SV. This is to be expected as a direct result of a high-energy proton's low LET producing a low-density ionization track as it traverses matter. Secondary electrons that are produced within the gas and traverse the SV can produce further ionizations within the DNA equivalent volume. It is the ionizations produced by these secondary electrons that create clusters larger than 1-2 ions within the SV. Assuming that we simulate the DNA, this means that secondary electrons are enhancing the biological damage produced by the primary particles.

We also studied the effect of Auger electrons on cluster size by including or excluding these electrons from the simulation. (see Fig. 6). It is clear that Auger electrons produced within the gas can cause further ionizations within the SV increasing the probability of larger clusters. However, this effect is quantitatively small when compared with the effect of all secondary electrons.

V. CONCLUSION

At this stage of our research, we have investigated the effectiveness of GEANT4 in obtaining incident beam data to achieve a simulated input for the nanodosimeter. This can then be processed by a special simulation code that transports protons and secondary electrons in propane in order to compute nanodosimetric cluster size distributions. The GEANT4 code provides a means for simulating the beam modifying devices that the radiation field must pass through before entering the nanodosimeter. This allows a more accurate assessment of the radiation field entering the nanodosimeter that should lead to a better agreement between experimental and simulated cluster size distributions. Some discrepancy was observed in comparison between the simulated and experimental mean cluster size and the cluster size distribution including zero-events. This is believed to be due to secondary particles produced in the up-stream beam modifying devices of the system, in particular, the silicon tracking detector located immediately in front of the gas volume. The propane simulation program in its present form is limited in that it can only account for one type of incident radiation, protons in this case. However, after passing through beam modification devices the radiation field will not only comprise of protons, but also neutrons and low-energy secondary electrons, which are likely to contribute to the additional clusters within the nanodosimeter observed experimentally.

In order to improve the accuracy of the nanodosimeter simulation program, particles such as neutrons and electrons entering the gas volume also need to be accounted for.

The importance of secondary electrons generated inside the nanodosimeter to cluster size was highlighted in this research. Secondary electrons are the main contributors to cluster sizes larger than two ions for 250 MeV proton irradiation. Auger electrons make a small contribution to larger cluster frequency.

These results have supported the program we have implemented into the investigation of nanodosimetry and its importance to radiation therapy and radiation protection. They have also highlighted the importance of accurate Monte Carlo simulations in further developments into experimental nanodosimetry.

VI. ACKNOWLEDGEMENT

Dr. Schulte's research is supported by the National Medical Technology Testbed Inc. (NMTB) under the U.S. Department of the Army Medical Research Acquisition Activity, Cooperative Agreement Number DAMD17-97-2-7016.

The authors would also like to acknowledge the support of the Australian Institute of Nuclear Science and Engineering (AINSE) and the Australian Nuclear Science and Technology Organisation (ANSTO), including the use of the high speed computer cluster located on site at ANSTO for Monte Carlo simulations of experiments.

VII. REFERENCES

- [1] American Cancer Society, Statistics for 2004, http://www.cancer.org/docroot/stt/stt_0.asp
- [2] Garty G., Shchemelinin S., Breskin A., Chechik R., Assaf G., Orion I., Bashkurov V., Schulte R., Grosswendt B., The performance of a novel ion-counting nanodosimeter, Nucl. Instrum. Meth. A 492, 2002, (1-2): 212-235.
- [3] Schulte R., Bashkurov V., Garty G., et al. Ion-counting nanodosimetry: current status and future applications. Australas. Phys. Eng. Sci. Med., 26, 140-146, 2003.
- [4] Hill MA. Radiation damage to DNA: the importance of track structure. Radiat Meas. 31, 15-23, 1999.
- [5] Geant4 User's Guide – For Application Developers, Geant4 User's Documents, March 2004
- [6] Geant4 Physics Reference Manual, Geant4 User's Documents, March 2004
- [7] National Institute of Standards and Technology (NIST) PSTAR Database Program, <http://physics.nist.gov/cgi-bin/Star/compos.pl?ap>